Studies on the behaviour of bottom structures during grounding

M.S. Samuelides
National Technical University of Athens, Zografos, Greece

J. Amdahl
Norwegian University of Science and Technology, Trondheim, Norway

R. Dow
University of Newcastle, Newcastle, UK

ABSTRACT: During that last twenty years there have been numerous procedures for the simulation of ship groundings. These are usually based on simplified assumptions that concern the loading of the ship bottom structure and the structural response modes. More recently the increase in the computing power have made possible the simulation of grounding using FE codes, which do not need an a priori assumption for the failure mode of the structural elements. However, other elements of the analysis, such as the description of the sea-bed and the modelling of the material are still under investigation and there have not yet been established guidelines for their inclusion in a grounding analysis. The paper presents an investigation of the loading patterns that are applied to the bottom structure during grounding, reviews and discusses analytical and numerical methods for grounding analysis, and compares the results of six methods when applied to simulate the grounding of a VLCC that occurred in 1975.

1 INTRODUCTION

According to Zhang (2002) the grounding rate for Ro-Ro and merchant navy ship types with lengths over 100 m, is 0.02 per ship year. That means that every second ship is expected to experience grounding in her life, assuming that the life of a ship is 25 years. The data refer to the years 1990 to1999 represent a sample of 1800 ship-years. Among the incidents, only one resulted in total loss, whereas all the other were recovered.

Using the reports of accidents occurred from 1993 to 2002, which refer to ships with Greek flag over 100GT, we obtained that during those 10 years 194 groundings were reported. The incidents occurred to Greek ships all over the world.

Taking into account the total Greek fleet over 100GT these years, we have concluded that the grounding rate per year vary from $3.56 \cdot 10^{-3}$ to $1.6 \cdot 10^{-2}$, whereby the average value is 0.01 per year ship. This value corresponds to a return period, which is twice as high as the return period obtained by the figures disclosed in Zhang (2002). It should be noted that the sample of the Greek fleet cover also ships that can be much shorter than 100 m, which is the lower limit of the ship size used in Zhang (2002). Among the 194 cases, two resulted in total loss. Three cases reported pollution, in one case a death was reported and in seventeen cases there was flooding of compartments. In the study that refers to Greek fleet, grounding incidents include all contacts with submerged stationary obstacles, and could have been caused by any reason, even intentionally grounding, when the captain wished to avoid more serious consequences.

Following a number of grounding incidents which caused serious consequences, there has been a major concern, to adopt appropriate measures in order to reduce the probability of grounding occurrence on one hand and to better understand the mechanics of the incident, so that it will be possible to design and build ships that have an acceptable behaviour in case they ground, on the other. Wang et al (2000) have investigated the behaviour of a double hull in a variety of grounding scenarios. A comprehensive survey of methodologies for the assessment of ships that ground is presented in ISSC (2006).

Rules for building vessels do not explicitly refer to grounding loads. Mitigation of the consequences of such accidents is usually achieved through defining a certain distance between inner and outer bottom, defining appropriate arrangement of cargo and fuel tanks and limiting their size IACS (2006).

The paper investigates the loading patterns that are applied to the bottom structure of a ship that grounds and the subsequent structural response/failure mechanisms. Existing methods to simulate the structural behaviour during grounding are reviewed and the results obtained from their application are compared.

2 LOADING PATTERNS DURING GROUNDING

In order to be able to simulate the response of the bottom structure of a vessel, when it contacts the sea bed it is essential to represent in a realistic manner the loading patterns that the bottom is subjected to. The section summarizes relevant observations from five grounding incidents, that have been reported in the literature and draws conclusions that are related to the loading of the bottom structure:

VLCC-January 1975: (Kuroiwa 1996, Pedersen et al 2000, Simonsen 1997b, Tikka 2000, Wang et al 1997, Zhang 2002)

On 6 January 1975 a one year old, single skin oil tanker having a length of 304 m and 273,000 dwt, rode over the Buffalo Reef off the coast of Singapore at a speed of 11.5 to 12 knots. The bottom of the ship was torn about from the bow for approximately 180 m along the centerline. The width of the opening varied between 2 and 5 m and the depth of the penetration has been reported to be 2 to 3 m. However, it is possible that the maximum penetration that was observed and that was 5 m, could have been caused after the initial grounding, when the ships sat for 10 days on the reef. The structures on the outer sides of the rupture were heavily concavely deformed toward the interior of the tanks. The width of the transverse frame deformation was reported to be approximately 7 m to 8 m.

El Paso Paul Kayser-1979:Poudret et al (1981)

The ship was a 130000m^3 and 98000 t membrane LNG carrier, which grounded in July 1979 on a rock near Gibraltar. Prior to grounding the speed of the vessels was estimated to be 18 knots, and the kinetic energy 4200 MJ. The grounding did not cause any leak of cargo and when the ship was inspected it was found that the length of damaged plates extended on a length of about 185 m port and 67 m starboard. Despite the fact that the ship was at the time of he incident at full speed, there has been to penetration of the cargo holds, not even of the double bottom. Figure 1, which has been reproduced from www (Juckett, 2002), shows the damage in the outer shell of the bottom structure.

Tanker Sea Empress-February1996

http://www.archive.official-documents.co.uk/ document/dot/seaemp/semp.htm

SEA EMPRESS, a single bottom tanker loaded with a cargo of 131000 t, grounded off the coast of south west Wales in February 1996. Although the main engine was stopped, put astern and both anchors dropped the vessel continued to run ahead and came to rest aground, approximately 5 cables northeast of the initial grounding position. The grounding caused rupture of the starboard side cargo and ballast tanks and a 2,500 t of crude oil was released to the sea. The vessel was guided into deeper water, but the ship grounded once more and for the next four days efforts by the salvors to regain control of the casualty were unsuccessful and the casualty went aground again on a number of occasions. It was not until seven days later that the casualty was successfully refloated and brought under control, and during that period, i.e. from the initial grounding until the vessels was refloated, the hull was subject to pounding damage. Figure 2 from the above mentioned site shows the damage of the bottom.

Navy vessel VALVIDIA-May 1997

http://www.shipstructure.org

VALVIDIA ran aground after an engine failure of Northern Chile, on May 1997. Subsequently the ship broached with the heading almost parallel to the beach because of breaking waves. Most of the bottom of the hull suffered some structural damage, but the presence of diesel and heavy surf limited diver accessibility for inspection. The consistent pounding of breaking waves caused

severe hull damage to 30 tanks. The hull girder experienced longitudinal buckling along the keel and the seaward sideshell. This buckling mode was caused by the load condition of having the hull supported by the beach on the port side, while the sea continuously impacted the starboard side.

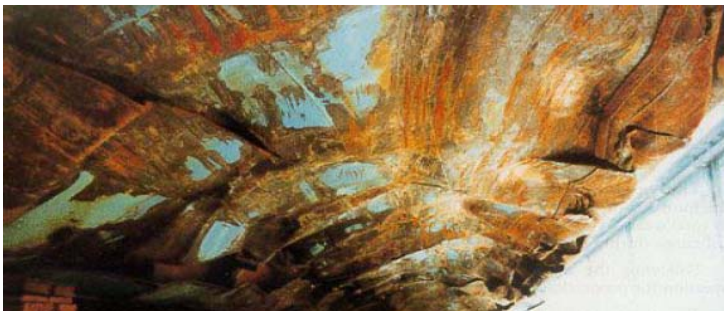
Figure 1: El Paso Paul Kayser


Figure2: Sea Empress

Bulk Carrier NEW CARISSA-February 1989 http://www.shipstructure.org

NEW CARISSA was a 195 m double bottom bulk carrier that was built in 1989. On February 4, 1999, the ship, carrying approximately 400,000 gallons (1500 tons) of fuel, grounded approximately 270 m off a beach north of Coos Bay, Oregon. Within a few hours, the vessel was fully broached to the incoming seas. For the three consecutive days the vessel experienced high winds with gusts up to 70 knots and sea swells measured from 5 m to 8.5 m. Further, the vessel was in the surf zone and it was subject to breaking waves, which were much higher than the measured sea swells. Four days after the initial grounding incident, the vessel began to leak oil and a salvage team onboard the vessel discovered that fuel tanks and ballast tanks below the two consecutive cargo holds, located forward of the engine room, were breached to the sea. Six days after the ship grounded the engine room flooded due to a major breach that was later determined to be from a fracture located on the lower portion of the forward engine room bulkhead and a 4.6 to 6.1 meters vertical fracture that appeared on the starboard side shell plating, at the adjacent cargo hold. The day after, subsequent to an attempt to burn the oil, which caused explosions, the vessel broke in half.

Conclusion

From the description of the above mentioned grounding incidents, we may draw the following conclusions regarding the loading of the bottom structure:

a) the bottom structure is subjected to a number of loading patterns, which depend, on the topology and type of sea bed and the impact geometry;
b) the loading due to grounding, is not limited in time only in the initial phase of a grounding incident, i.e. when the kinetic energy of the ship prior to grounding is dissipated in structural energy, but may damage the ship's structure days after the incident;
c) structural components that are damaged during the initial incident, may subsequently be subject to serious loading conditions, which may cause further damage.

A common loading pattern when a ship runs with forward speed on the sea bed is a contact force distribution, which is oblique with respect to the plane of the bottom shell. The figures of the damaged hulls of Sea Empress and El Paso Paul Kayser reveal that the shell of the vessels were subject to such type of loading while they were moving forward in contact with rocks. In the case of Sea Empress (Fig. 2) the side shell has been removed from the action of the rock, while in the case of El Paso Paul Kayser (Fig. 1) it appears that the side shell was pushed inside the double bottom space.

The bottom structure may also be subject to transverse loading, when the ship moves vertically towards the sea bed, a mode that may occur statically or dynamically: such a transverse load is static when the ship sits on a pinnacle, which supports its weight, and dynamic in case the ship is relatively light and the wave action causes a repeated impact of the bottom to the sea bed (pounding impact). The VLCC that was previ-

ously discussed seems to have suffered from transverse static load on the double bottom structure, while New Carissa suffered from pounding impact. Transverse loading on the bottom plate also occur when the ship moves towards to the sea bed as a result of tidal actions. When the load to the bottom is transverse and the ship does not move horizontally, the bottom structure – girders and floors –suffer from crushing.

Loading on structural elements of the hull of a ship that rests on the sea bed may also result from hull bending either in the horizontal plane or in the longitudinal plane of symmetry of the vessel. The latter is the result of wave action on the hull, but it may also occur when the ship rests on a projection of the sea bed. In the case of New Carissa, for example, scouring action developed a pinnacle under the vessel's amidships, which caused hogging stresses to the ship's hull. Horizontal bending, such as the bending of Valvidia, results from the wave action on a side of a vessel, which is supported by the sea bed on her opposite side. In this case each wave impact caused bending that created compressive stresses on the side that is subjected to impact and tension on the opposite side. The side subjected to impact may suffer from buckling.

3 ANALYTICAL PROCEDURES FOR GROUNDING INVESTIGATIONS

The mode that has drawn much attention among researchers that have addressed the structural behaviour of ships that ground, is the resistance of the bottom plate to tearing by a wedge. Relatively simple formulae have been developed to simulate this mode of response by Wierzbicki et al (1993), Paik (1994), Ochtsubo at al (1995), Wang et al (1997) and Zhang (2002). Among those, the formulation of Paik (1994) is empirical, i.e. it is based on test results, whereas the other three have been derived on the basis of assumed modes of deformation. All four formulae propose that the resistance of the plate to tearing is proportional to the flow stress of the material. Further the cutting force is proportional to the 1.5 or 1.6 power of the area-equivalent thickness of the plating, and the 0. 4 to 0.5 power of the cutting length, i.e. the length of the penetration of the cutting object to the plating. The formula of Wierzbicki (1993) involves a parameter involving the Crack Opening Displacement (COD) and that of Zhang (2002) the failure strain of the material. The other two do not involve implicitly any material property relevant to failure. The tearing resistance according to the methods presented in the paragraph, depends on the depth of penetration of the tearing object within the plate and therefore they do not predict a constant tearing force, which would develop in a steady sate solution. According to Wang et al (1997) the steady-state force could be predicted if the cutting length is substituted by the length of the tearing object. All four formulae are presented in Table 1. Zhang (2002) has compared results obtained by the application of the formulae and concluded that when the wedge angle is small, i.e. less than 40 the comparison is good.

TABLE 1: TEARING RESISTANCE OF PLATES CUT BY A WEDGE

Wierzbicki et al (1993)	$F_R = 3.28 \cdot \sigma_F \cdot t^{1.6} \cdot \mu^{0.4} \cdot \bar{\delta}_t^{\,0.2} \cdot l^{0.4}$
Paik (1994)	$F_R = 1.5 \cdot \left(3.76 \cdot \theta^2 - 1.156 \cdot \theta + 1.112\right) \cdot \sigma_F \cdot t^{1.5} \cdot l^{0.5}$
Wang et al (1999)	$F_R = 1.51 \cdot \sigma_F \cdot t^{1.5} \cdot l^{0.5} \cdot \sqrt{\sin\theta} \cdot \left(1 + \frac{\mu}{\tan\theta}\right)$
Zhang (2002)	$F_R = 1.942 \cdot \sigma_F \cdot t^{1.5} \cdot l^{0.5} \cdot \varepsilon_R^{\,0.25} \cdot \sqrt{\tan\theta} \cdot \left(1 + \frac{\mu}{\tan\theta}\right)$

σ_F: flow stress, which is taken as the average of the yield and ultimate stress, t: equivalent thickness, i.e. area of cross section of plate with longitudinals, divided by the width, θ: half angle of wedge shaped tearing object, which is taken as when the tearing object is conical, μ: friction coefficient assumed to be 0.3 to 0.4, l: tearing length (for the calculation of the steady state cutting force it is taken equal or twice the length of the tearing object), ε_R: uniaxial rupture strain.

$\bar{\delta}_t$, dimensionless crack opening displacement parameter, which is the ratio of Crack Opening Displacement (COD) over plate thickness and assumed to be equal to 1.

Further modes of response of structural components during grounding have been investigated by Simonsen (1997a), Wang et al (1997) and Midtun (2006). Simonsen (1997a) has developed an analytical methodology for the calculation of the resistance of plate elements under transverse loading, and the resistance of longitudinal elements under in plane loading. Wang et al (1997) included in the grounding resistance of a bottom structure, the resistance of transverse members and the resistance of the bottom plating to concertina tearing. Midtun (2006) studied the response of a longitudinal bottom girder, when it is struck by the oblique surface of a rigid object moving along the longitudinal direction of the girder. The model of Midtun is discussed in following sections.

4 NUMERICAL SIMULATIONS OF GROUNDING RESPONSE

Numerical simulations of grounding response are performed by employing FE codes (see for example Kuroiwa (1996) and Zhang at al (2006). Paik (2007) has also suggested a simplified code for the simulation of such incidents. However, despite the increase in the computing power, which simplifies the FE simulations of large scale problems, there are still problems that need to be resolved in order to obtain credible results. The problem that is currently widely discussed is that of the failure criterion of the material. The simplest way to account for material failure is to define a limit to the Mises strain as this is calculated from the FE codes. However, such a threshhold value (usually referred to as "rupture strain"), which is usually defined on the basis of uniaxial tension tests have shortcomings: a) there is no evidence that the threshold value of the Mises strain is the ultimate strain measured during uniaxial tensile tests, b) the Mises strains developed within an element, in a region where the spatial variation of strain is strong, depend highly on the element size, and c) the application of the Mises law disregards the effect that is caused by hydrostatic pressure, i.e. the first invariant of the stress tensor. To overcome some of the problems Germanischer Lloyd proposed a formula to relate the rupture strain to the element size. In particular, the rupture strain ε_R is given by the formula: $\varepsilon_R = 0.056 + 0.54 \cdot (t/l)$ for shell elements and $\varepsilon_R = 0.079 + 0.76 \cdot (t/l)$ for beam elements, whereby l, t is the length and thickness of the element. Paik (in press) proposed to define the rupture strain from the formula: $\varepsilon_R / \varepsilon_{UR} = 4.1 \cdot (t/l)^{0.58}$, where ε_{UR} is the nominal fracture strain obtained by tensile coupon tests. If the latter is assumed to be 10%, then Figure 3 below shows a comparison between the values of the rupture strains, obtained by the formulae of GL and Paik for element size between 20 and 50 mm, which is usual for grounding applications.

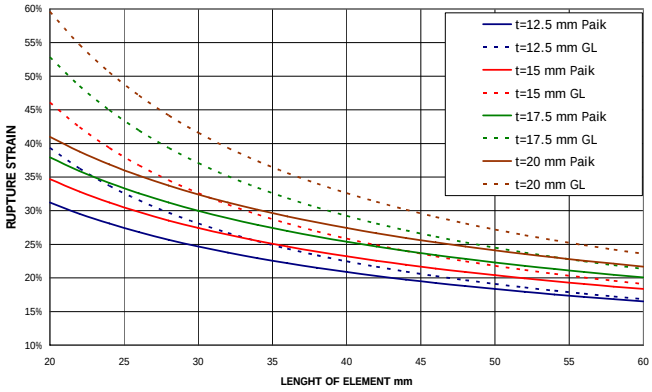

Figure 3: Maximum allowable strain

A rupture criterion that takes into account the triaxiality of the stress field has been proposed by Johnson and Cook (1985). The authors propose that the ultimate plastic strain of the material is a function of the ratio of the first invariant of the stress tensor, i.e. the hydrostatic pressure, over the Mises stress, and give the material constants that are needed for the application of the criterion for a high tensile steel. However it was not possible to find in the literature the parameters that are needed to implement the criterion for mild steel. Servis & Samuelides (2006) have used the T-failure criterion that correlates the reversible elastic energy density storage with material failure. This criterion was developed at the National Technical University of Athens and is currently used to predict the initiation of pre-existent macroscopic cracks, as well as in the calculation of forming limit diagrams (FLDs) for metal forming processes. The T criterion is based on two threshhold values of the density of the elastic strain energy stored during the loading process: an upper limit of the elastic energy density due to change in shape, the distortional energy, and an upper limit of the elastic energy density due to volume change, the dilatational energy. The distortional energy represents the energy stored in the material only in the case of pure shear and is the area under the Mises stress-strain (σ-ε) curve. The dilatational energy represents the energy stored in the material as a result of the hydrostatic loading, and it is the area under the p-Θ curve, where p is the hydrostatic pressure (first invariant of stress tensor), and Θ is the volume change. The volume of material is considered to have failed by extensive plastic flow when either the distortional energy or the dilatational energy reaches a critical value. The two critical values are material constants, independent of the shape of the volume of material and the induced loading, but depend on the strain rate and temperature. The definition of a threshhold value for the dilatational energy accounts for the effect of hydrostatic pressure in the material failure, a feature which is not taken into account by the von-Mises yield law. The au-

thors have proposed a procedure to estimate the critical values of the energy on the basis of torsion and uniaxial tensile tests and incorporated the failure criterion in FE code Abaqus/explicit to simulate the quasi-static tests reported in Paik et al (1999) (Fig. 4). The results in terms of force versus penetration is presented in Figure 5.

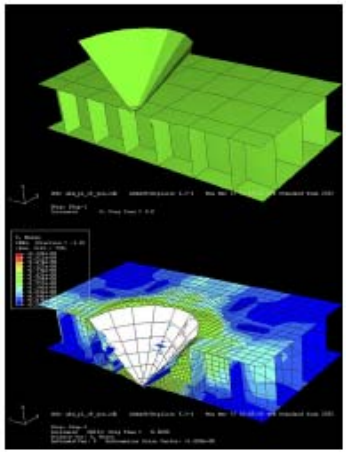

Figure 4: FE model of double side structure

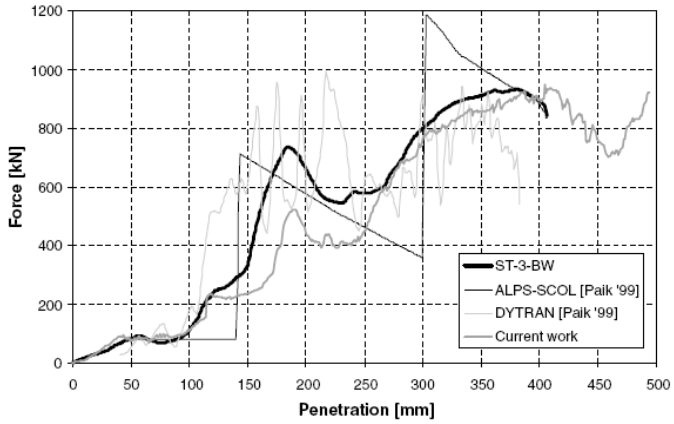

Figure 5: Experimental and theoretical results according to Paik et al (1999) and Servis et al (2006).

5 RESISTANCE OF LONGITUDINAL GIRDERS

Apart fr0m the shell plating longitudinal girders are key structural components in ship bottoms as concerns the resistance to grounding actions. The structural behaviour of longitudinal girders during grounding is quite poorly understood, and the deformation pattern and associated energy dissipation of girders were therefore subjected to a comprehensive study by Midtun (2006).

Initial simulations were carried out with the FE code LS_DYNA, where the girder is assumed to be deformed to a certain depth as the indenter representing the sea floor obstacle travels along the girder. The process is illustrated in Figure 6.

The girder is assumed to be continuous and long. The height of the girder web is h_w = 0.45 m and 0.9 m, the length is 8 m, the thickness varies with t = 8 – 16 mm.

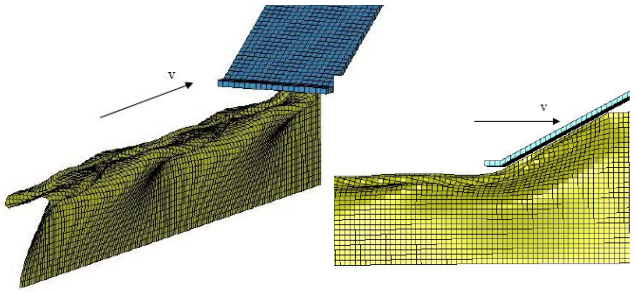

Figure 6: Deformation of girder subjected to travelling obstruction (h_w = 0.45 m, t = 12 mm).

The girder is un-stiffened and transverse girders are not included, initially. It is fixed in inner bottom (lower end in figure). A small part of the outer shell plating shell ("top flange") is modelled. It is fixed with respect to motion in the transverse direction, but free to move in the axial and lateral direction. (The outer shell is removed in most plots for visualization purposes). The indenter representing the sea floor is modelled as a plane object oriented at a certain angle of attack, φ, to the shell plating. The indenter is forced to move along the girder with a constant indentation depth, Δ. Friction is disregarded in the simulations. The material is assumed to be linear elastic and a (relatively) small linear hardening.

Figure 7 shows the deformation pattern for three different indentation depths. The apparent fold length increases with increasing indentation, but this is at least partly due to incomplete folding for small indentation depth, as observed from the cross-sectional view for Δ = 80 mm. Figure 8 shows the effect of varying the angle of attack for a constant indentation Δ = 160 mm. It is observed that when the angle increases the fold wave length is reduced, in both the axial direction and the vertical direction. The height of the girder web being deformed is also reduced.

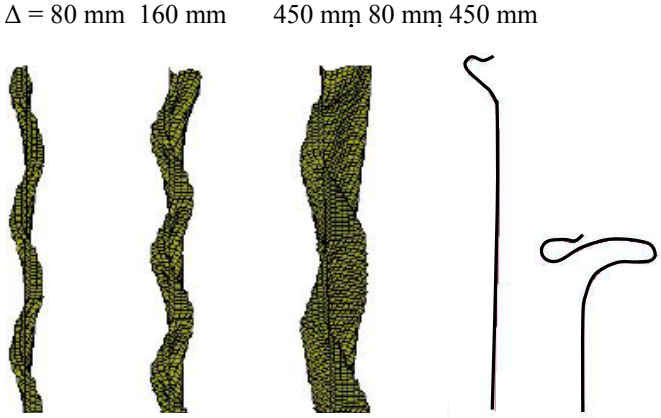

Figure 7: Deformation pattern and cross-sectional view for different indentations (h_w = 0.9 m, t = 12 mm, φ = 28^0).

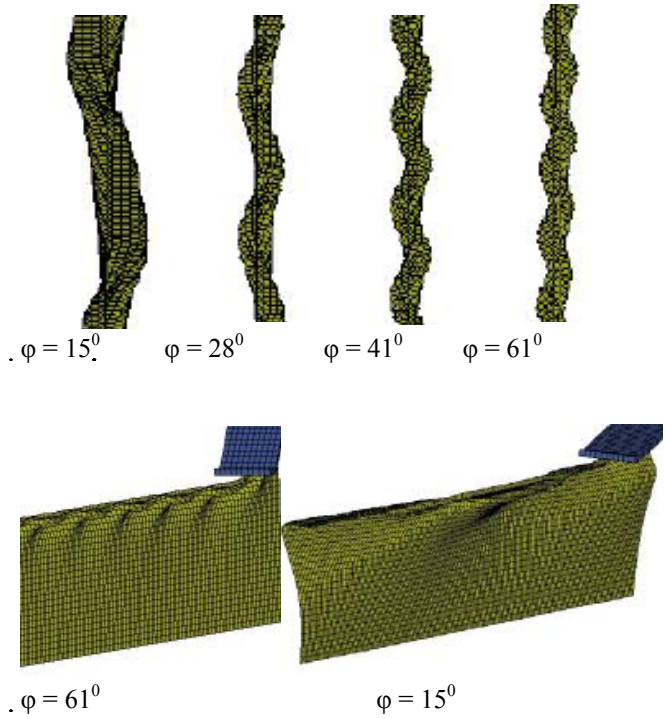

Figure 8: Deformation pattern for different angles of attack (h_w = 0.9 m, t = 12 mm, Δ = 160 mm).

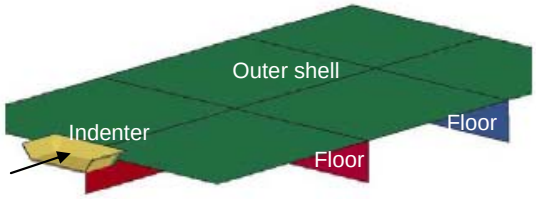

Figure 9: Longitudinal girder with floors and shell plating.

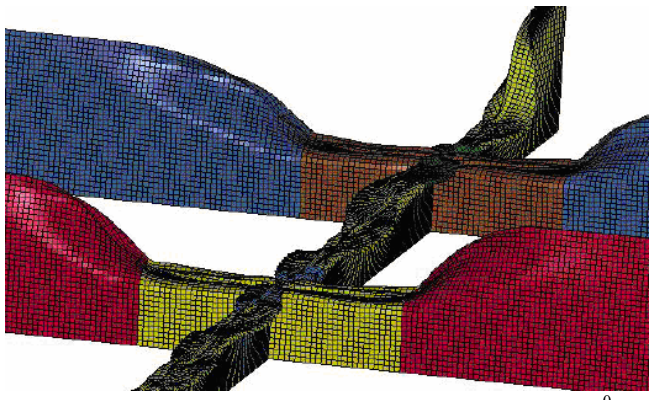

Figure 10: Deformed girders for Δ = 450 mm and φ = 51.3⁰.

In order to study the effect represented by transverse members, two intersecting floors were modeled. A larger part of the shell plating was also included in the model, illustrated in Figure 9. The distance between the floors is 4.2 m, the height is 0.9 m and the web thickness is 12 mm. Figure 10 shows an example of the deformation pattern for indentation Δ = 450 mm and attack angle φ = 51.3⁰. The shape of the indenter dictates very much the deformation pattern, which does not extend significantly outside the part in direct contact with the indenter. The same folding pattern as for the simple girder is observed. The folds seem to displace to the same side at before and after the intersection.

Although the pattern does not change when the floors are present, an important difference is noticed: The length of the fold increases. Figure 11 shows the deformation pattern in the longitudinal girder, for the bottom structure and the single girder. The attack angle and the indentation are not exactly identical (Δ = 150 mm, φ = 51.3⁰ (bottom structure) Δ = 160 mm, φ = 53,1⁰ (single girder)), but the difference cannot be explained by this small difference. Most likely the fold length increase is due to the confinement effect of the outer shell. The outer shell tends to displace in the axial direction along with the motion of the indenter. In the case of the single girder, the plating is free in the axial direction and does resist this motion very little. In the bottom structure, the axial motion is resisted by the adjacent shell plating, which causes large shear/tension strains to develop. The effect of this restraint is the same as reducing the angle of attack in case of the single girder (whereby the axial motion diminishes). Midtun (2006), further investigated the effect of including stiffeners on the floors and girders. Figure 12 shows the deformation pattern with vertically stiffened floors. The conclusion is that the stiffeners play a moderate role. Vertical stiffeners influence the deformation pattern significantly more when the floor/girder intersection is subjected to "axial" (vertical) crushing. When the girder is deformed by a moving indenter, the longitudinal deformation of the plating described above produces a significant out of plane deformation of the intersection. Consequently the deformation mode for a stiffened and unstiffened floor becomes quite similar.

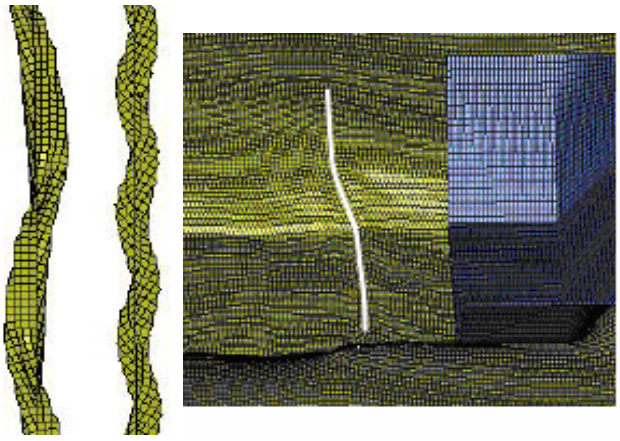

Figure 11: Deformation pattern in longitudinal girder as part of bottom structure (left), single girder (middle). Deformation in shell plating (right) viewed from below.

Longitudinal girders are typically fitted with horizontal stiffeners. Simulations show that their constraint and, hence, contribution to the resistance is limited.

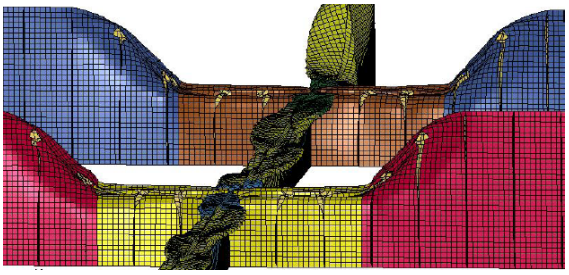

Figure 12: Deformation pattern with vertically stiffened floors.

Example of force deformation curves for the bottom model with no stiffeners on longitudinal girders, and with indentation Δ = 450 mm are shown in Figure 13. The horizontal component increases with large attack angles, such that the resultant force is normal to the contact plane. In the simulation only the horizontal force component contributes to the work. The passage of a frame by the indenter is expressed by a significant increase of the force level; between transverse frames it is fairly constant. The shape of the curve indicates that mechanism type of analysis of the average force during deformation of longitudinal girders and crushing of intersecting floors is possible.

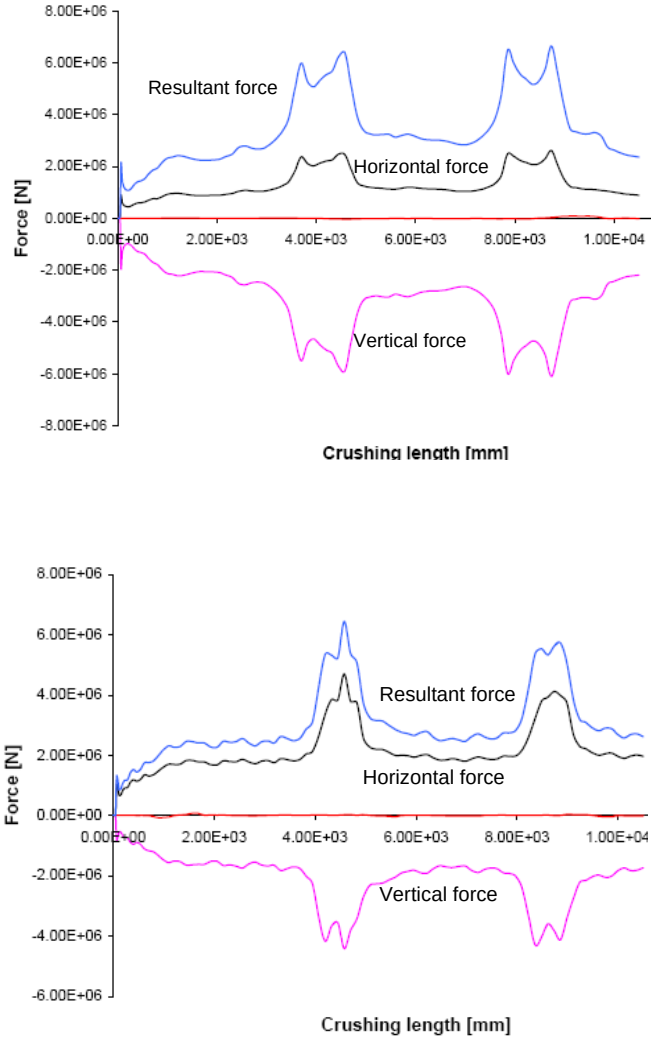

Figure 13: Force deformation curves for bottom structure with $\varphi = 24.4^0/51.3^0$ and Δ = 450 mm.

Midtun analysed the resistance to penetration of the girder web also by constructing folding mechanism. For illustration purposes use of paper models is beneficial (Fig. 14). Initially, it is assumed that the web yields by vertical deformation and the rectangular section in the web deforms into a parallelogram.

Once the deformation field is determined, the average resistance for complete folding of one wave can be calculated by means of the virtual work principle, taking into account the contributions from continuous deformation fields and bending about stationary yield lines. The mechanism shown in Figure 14 is compatible with a shear and axial compression field imposed on the rectangles. The length and width of the rectangle are unknown. If this can be determined by analytical minimization, the problem is easily solved. Unfortunately, for the problem it is not feasible. This indicates that the mechanism is not entirely correct. Later, Midtun concluded that the axial displacement observed in the numerical simulation should be included in the model. Nevertheless, using empirical values for the unknown parameters, the prediction of energy levels were not out of range. Generally the force level is unpredicted.

As to the energy dissipation on the floors Midtun concluded that in the central section subjected to uniform compression the resistance could adequately be predicted by means of formulas for axial crushing of cruciform sections. Outside central region, the Midtun used the method proposed by Simonsen (1997a). Compared to the single girder case, better agreement between numerical and analytic predictions is obtained for the longitudinal girder.

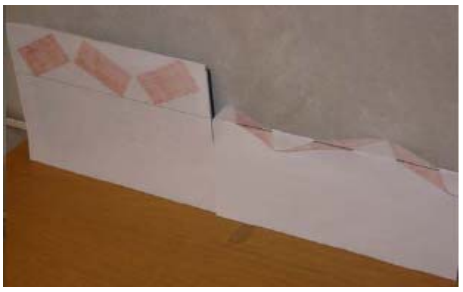

Figure 14: Paper model of folding mechanism.

6 INVESTIGATION OF GROUNDING INCIDENTS

The section presents the comparison of the results, which were obtained by the application of FE and analytical methods to simulate the grounding of the VLCC on the Buffalo Reef, and have been reported in the literature. The first analysis of the incident was reported by Kuroiwa (1996). The author performed a finite element analysis that took into account both the structural response of the bottom structure and the vertical motion of the vessels during the grounding. The longitudinal reaction force

was found at the initial stages of the grounding to have a peak of 60 MN. After the rupture of the collision bulkhead the resisting force varied between 16 MN and 35 MN, whereby the maxima occurred when the transverse frames provided maximum resistance. The computations showed a large vertical force which reached 80 MN and lifted the ship upwards during the incident. As a result of the lift the tip of the rock moved towards the bottom plate as the ship moved forward on the rock: thus, the penetration of the rock in the hull decreased to 2.25 m from 3 m, which was estimated when the hull came in contact with rock. According to the authors the damage length predicted by the analysis was 12 m longer than the actual damage length.

Simonsen (1997b) applied a procedure presented in Simonsen (1997a) in order to investigate the same accident. The author obtained the damage length as a function of the rock penetration, and he concluded that the observed damage length of 180 m corresponded to a rock penetration of 4.4 m, at the aft end of the damage. However the penetration that was observed 10 days after the incident was 5 m, which corresponds to a damage length of 150 m. The author claims that the penetration, which occurred during grounding should be less than 5 m and that the penetration increased during the 10 days, when the ship remained on the rock, as a result of transverse loading exerted by the rock to the bottom structure.

A further investigation of the accident has been reported by Tikka (2000). The investigation used the computer code DAMAGE that is based on the theory developed by Simonsen (1997a). The application of the program predicted a damage length of 177 m. This results compares extremely well with the observed damage of 180 m, but it shows sensitivity to the eccentricity of the rock at the time of the incident, a parameter which, according to the author is not known. The estimated vertical and horizontal forces for 15 sec from the first contact varied almost linearly from 33 MN to 50 MN.

The grounding was also analyzed by three simplified methods developed by Wang et al (1997), Pedersen et al (2000) and Zhang (2002).

The methodology of Wang et al (1997) is based on the calculation of the energy that is absorbed by tearing of bottom plates (see previous section Table 1) as the rock moves in the longitudinal direction, the energy absorbed by the transverses as they deform out of plane and the energy absorbed by the area of the bottom plate which is adjacent to the final position of the rock and which heavily deformed out of plane. Depending on the mode of tearing of the bottom shell –tearing or concertina tearing- and the assumed width of the rupture, the authors calculated that the energy absorbed in the damaged bottom structure was 83% to 115% of the kinetic energy of the ship prior to grounding. For the estimation of the kinetic energy the speed of the ship was taken equal to 11.5 knots and the added mass coefficient 5%. The authors do not give the mass of the vessel prior to impact which according to (Kuroiwa 1996) is 273000 t. On the basis of the above data and results, we may calculate the mean force that resists the damage, by dividing the energy absorbed according to the calculation, by the damage length i.e. 180 m. From the calculations we obtain that the resisting force is between 23 MN and 32 MN depending on the tearing mode and the width of rupture that have been assumed.

Pedersen et al (2000) proposed the following formula relating the energy absorbed by the structure E_s with the volume of the damaged material R_T

$$E_S = 3.21 \cdot \left(\frac{t}{b}\right)^{0.6} \cdot \sigma_F \cdot R_T$$

where σ_F is the flow stress of the material, t is the equivalent plate thickness and b the critical tearing length, where the steady state has been reached, which is taken as the width of the tearing object or damage width. By dividing the above energy by the damage length, we obtain the mean resisting force F_s, which is equal to:

$$F_R = 3.21 \cdot \left(\frac{t}{b}\right)^{0.6} \cdot \sigma_F \cdot t \cdot b$$

If we apply this formula, using the data that were reported in Wang (b=5 m, t=56.5, σ_0=320MPa) we obtain that the mean resisting force equals to 20MN. If the damage width is taken equal to 7 m, as it appears to be at certain locations, the resisting force equals to 23 MN.

Finally Zhang (2002) proposed a formula for the calculation of the mean resisting force F_R during damage, which relates the resisting force to the flow stress, the equivalent thickness of the bottom plate including longitudinals t, the equivalent thickness of the bottom plating including longitudinal and transverses t_e and the damage width b:

$$F_R = 3.58 \cdot \sigma_F \cdot t_e \cdot t^{0.6} \cdot b^{0.4}$$

The author applied the formula and calculated that the resisting force equals to 28.2 MN.

Discussion

From the description of the actual grounding given in the various publications it is concluded that at the time of grounding the ship had a displacement of 273000 t and a speed of 11.5 to 12 knots. Thus the kinetic energy of the ship prior to impact was 4777 MJ to 5202 MJ if we ignore the added mass and 5016 MJ to 5462 MJ if the added mass is taken equal to 5%. The corresponding mean resisting force, which is the energy divided by the damage length, i.e. 180 m, varies from 26,5 MN to 28,9 MN if the added mass is neglected and from 27.9 MN to 30.3 MN if the added mass is 5%.

If we compare the forces that have been obtained from the simulations with the average resisting force according to the preceding paragraph, the closest estimation is obtained by the formula of Zhang (2002). The numerical simulation of Kuroiwa (1996) yields also a non-steady force (from 16 MN to 35 MN) that fluctuates around the value of the average force as obtained by the test results. The procedure of Simonsen as applied in (Simonsen 1997b) or (Tikka 2000) gives a damage length that compares well with that measured after the grounding.

7 CONCLUSIONS

Grounding is a complicated phenomenon that involves a number of energy absorbing mechanisms. Further the structural response of the hull depends on the relative position of the ship to the obstacle or obstacles that come in contact with the hull, their shape and rigidity. The damage due to grounding is not limited during the initial phase of the incident but continues while the ship rests on the sea bed.

During the last couple of decades, various methods for grounding have been developed and tested versus experimental results of results obtained from grounding incidents. FE methods have been also employed for a more comprehensive simulation of the phenomenon. However the results of the simulation of an actual grounding, still depends on assumptions, which are not always justified.

In order to establish a comprehensive procedure for grounding analysis, there is a need to understand the loading patterns, to which the bottom structure is subject, and the subsequent failure mechanisms. Relevant useful conclusions may be drawn from inspecting damaged hulls from ships that have experienced grounding. Thereafter it would be possible to reproduce the failure modes using FE codes. A major breakthrough would be achieved when it will be possible to define a realistic failure criterion for the material. Taking into account the various failure mechanisms it might be possible to define a failure criterion for each failure mode.

ACKNOWLEDGEMENTS

The work has been performed in the scope of the project MARSTRUCT, Network of Excellence on Marine Structures, (www.mar.ist.utl/marstruct/), which has been financed by the EU through the GROWTH Programme under contract TNE3-CT-2003-506141. Part of the contribution of the first author, has been performed during a visit to the Dep. of Naval Architecture and Ocean Engineering of Pusan National University, which was supported by the Korea Research Foundation and The Korean Federation of Science and Technology Societies.

REFERENCES

Germanischer Lloyd. Development of explanatory notes for harmonized solas chapter ii-1, International Maritime Organization (IMO).

IACS 2006. Common Structural Rules for Oil Tankers, Section 5/3.1.3

ISSC 2006. Report of Technical Committee V.1: Collision and Grounding. Proceeding of the 16th International Ship and Offshore Structures Congress, University of Southamtpon.

Johnson G.R. & Cook, W.H. 1985. Fracture Characteristics of Three Metals Subjected to Various Strains, Strain-Rates Temperatures and Pressures. Engineering Fracture Mechanics 21(1):31-48.

Juckett, D. 2002. Properties of LNG. US Department of Energy.

Kuroiwa, T. 1996. Numerical Simulation of Actual Collision and Grounding Experiments. In proceeding of conference on Design and Methodologies for Collision and Grounding Protection of Ships, SNAME:

Midtun, H.O. 2006. Analysis of tankers during grounding and collision. Master Thesis, Norwegian University of Science and Technology.

Ohtsubo H. & Wang G. 1995. An upper-bound solution to the problem of plate tearing. J Mar Sci Technol 1:46–51.

Paik J.K. (1994). Cutting of a longitudinally stiffened plate by a wedge. J Ship Res 38(4):340–348.

Paik, J.K. in press. Practical Techniques for Finite Element Modeling to Simulate Structural Crashworhtiness in Ship Collisions and Grounding – Part I Theory. Ships and Offshore Structures.

Paik J.K., Chung J.Y., Choe I.H., Thayamballi A.K., Pedersen P.T. & Wang G. 1999. On rational design of double hull tanker structures against collision. In The Society of Naval Architects and Marine Engineers, 1999 annual meeting, Paper Number, 14.

Paik, J.K. and Seo, J.K. 2007. A Method for Progressive Structural Crashworthiness Analysis under Collisions and Grounding. International Conference on Advancements in Marine Structures, 12-14 March, Glasgow, UK.

Pedersen, T. & Zhang, S. 2000. Absorbed Energy is Ship Collisions and Grounding – Revising Minorsky's Empirical Method. Journal of Ship Research 44(2):140-154.

Poudret, J., Huther, M., Jean, P. & Vauhan, H. 1981. Grounding of a Membrane Tanker; Correlation Between Damage Predictions and Observations. Extreme Loads Response Symposium, Arlington, VA.

Servis, D. & Samuelides M. 2006. Implementation of the T-failure criterion in finite element methodologies. Computers & Structures 84:196-214.

Simonsen B.C. 1997a. Ship Grounding on Rock I. Validation and Application, Marine Structures 10:563-584.

Simonsen B.C. 1997b. Ship Grounding on Rock II. Validation and Application. Marine Structures 10:563-584.

Tikka, K.K. 2000. Risk-based Life Cycle Management of Ship Structures. Ship Structures Committee Report SSC-417.

Wang, G., Arita, K. & Liu, D. 2000. Behaviour of double hull in a variety of stranding or collision scenarios. Marine Structures 13(3):147-187.

Wang G., Ohtsubo, H, & Liu, D. 1997. A Simple Method for Predicting the Grounding Strength of Ships. J Ship Res 41(3):241-247.

Wierzbicki T. & Thomas P. 1993. Closed-form solution for wedge cutting force through thin metal sheets. Int J Mech Sci 35:209-229.

Zhang, A. & Suzuki, K. 2006. Dynamic FE simulations of the effect of selected parameters on grounding test results of bottom structures. Ship and Offshore Structures 1:117-125.

Zhang, S. 2002. Plate tearing and bottom damage in ship grounding. Marine Structures 15:101-117.